NPS-MV-01-001

# NAVAL POSTGRADUATE SCHOOL
# Monterey, California

**Real-Time Tracking and Display of Human Limb Segment Motions Using Sourceless Sensors and a Quaternion-Based Filtering Algorithm – Part I: Theory**

by

Robert B. McGhee
Eric R. Bachmann
Xiaoping Yun
Michael J. Zyda

November 2000

Approved for public release; distribution is unlimited.

Prepared for: NPS Moves Academic Group

| **REPORT DOCUMENTATION PAGE** | Form approved<br>OMB No 0704-0188 |
|---|---|

**Public reporting burden for this collection of information is estimated to average 1 hour per response, including the time for reviewing instructions, searching existing data sources, gathering and maintaining the data needed, and completing and reviewing the collection of information. Send comments regarding this burden estimate or any other aspect of this collection of information, including suggestions for reducing this burden, to Washington Headquarters Services, Directorate for information Operations and Reports, 1215 Jefferson Davis Highway, Suite 1204, Arlington, VA 22202-4302, and to the Office of Management and Budget, Paperwork Reduction Project (0704-0188), Washington, DC 20503.**

| **1. AGENCY USE ONLY (Leave blank)** | **2. REPORT DATE**<br>November 2000 | **3. REPORT TYPE AND DATES COVERED**<br>Technical Report |
|---|---|---|

| | |
|---|---|
| **4. TITLE AND SUBTITLE**<br>Real-Time Tracking and Display of Human Limb Segment Motions Using Sourceless Sensors and a Quaternion-Based Filtering Algorithm – Part I: Theory | **5. FUNDING**<br>N6M ARO |
| **6. AUTHOR(S)**<br>McGhee, Robert B., Bachmann, Eric R., Yun, Xiaoping, and Zyda, Michael J. | |
| **7. PERFORMING ORGANIZATION NAME(S) AND ADDRESS(ES)**<br>Naval Postgraduate School<br>Monterey, CA 93943-5118 | **8. PERFORMING ORGANIZATION REPORT NUMBER**<br>NPS-MV-01-001 |
| **9. SPONSORING/MONITORING AGENCY NAME(S) AND ADDRESS(ES)** | **10. SPONSORING/MONITORING AGENCY REPORT NUMBER** |

**11. SUPPLEMENTARY NOTES**
The views expressed in this thesis are those of the author and do not reflect the official policy or position of the Department of Defense or the U.S. Government.

| **12a. DISTRIBUTION/AVAILABILITY STATEMENT**<br>Approved for public release; distribution is unlimited. | **12b. DISTRIBUTION CODE** |
|---|---|

**13. ABSTRACT (Maximum 200 words.)**
Recently, a new impetus has been given to work to produce a whole body human/computer interface system, which encumbers the wearer to a minimum degree and operates over long distances. The input portion of such an interface can be derived by appropriate processing of signals from a nine-axis sensor package consisting of a three-axis angular rate sensor, a three-axis magnetometer, and a three-axis linear accelerometer. This paper focuses on data processing algorithms for MARG sensors. Since human limb segments are capable of arbitrary motion, Euler angles do not provide an appropriate means for specifying orientation. Instead, quaternions are used for this purpose. Since a quaternion is a four-dimensional vector, and a MARG sensor produces nine signals, this data processing problem is "overspecified". This fact can be used to discriminate against sensor noise and to reduce the effects of linear acceleration on measurement of the gravity vector by accelerometers. Detailed computer simulation studies and the results of preliminary experiments with a prototype body tracking system confirm the effectiveness of the quaternion body-tracking filter.

| | |
|---|---|
| **14. SUBJECT TERMS**<br>Inertial Tracking, Magnetic Tracking, MARG Sensors, Complementary Filtering, Quaternions | **15. NUMBER OF PAGES**<br>27 |
| | **16. PRICE CODE** |

| **17. SECURITY CLASSIFICATION OF REPORT** | **18. SECURITY CLASSIFICATION OF THIS PAGE** | **19. SECURITY CLASSIFICATION OF ABSTRACT** | **20. LIMITATION OF ABSTRACT** |
|---|---|---|---|
| Unclassified | Unclassified | Unclassfied | UL |

**NSN 7540-01-280-5800** **Standard Form 298 Rev. 2-89)**
**Prescribed by ANSI Std 239-18**

NAVAL POSTGRADUATE SCHOOL
Monterey, California 93943-5000

RADM David R. Ellison, USN
Superintendent

Richard Elster
Provost

This report was prepared for __NPS_MoVES Academic Group___________________________
and funded by _Army Research Office (ARO), Modeling and Simulation Office (N6M)

This report was prepared by:

Robert B. McGhee
Professor

Eric R. Bachmann
Research Assistant Professor

Xiaoping Yun
Professor

Michael J. Zyda
Professor

Reviewed by:

Michael J. Zyda
Chair, MoVES Academic Group

Released by:

D. W. Netzer
Associate Provost and
Dean of Research

*Submitted to Presence, May, 2001*

# Real-Time Tracking and Display of Human Limb Segment Motions Using Sourceless Sensors and a Quaternion-Based Filtering Algorithm – Part I: Theory

R.B. McGhee, E.R. Bachmann, X.P. Yun, and M.J. Zyda

Naval Postgraduate School, Monterey, CA93943
E-mail: mcghee@cs.nps.navy.mil

## Abstract

*Tracking and display of human limb segment motions has been the topic of much research and development over many years for purposes as varied as basic human physiological studies, physical rehabilitation, sports training, and the construction of anthropomorphic robots. More recently, a new impetus has been given to such work by the desire to produce a whole body human/computer interface system, which encumbers the wearer to a minimum degree and operates over long distances. The input portion of such an interface can be derived by appropriate processing of signals from a nine-axis sensor package consisting of a three-axis angular rate sensor, a three-axis magnetometer, and a three-axis linear accelerometer. In this paper, such a sensor system is called a MARG (Magnetic field, Angular Rate, and Gravity) sensor. Recent advances in micromachining (MEMS) technology, and magnetometer miniaturization, have allowed the development of MARG sensors of very small size, suitable for attachment to individual human limb segments. At the same time, advances in wearable computers and wireless data communication techniques make it feasible to begin the development of a practical full body tracking system using sourceless MARG sensors.*

*This paper focuses on data processing algorithms for MARG sensors. Since human limb segments are capable of arbitrary motion, Euler angles do not provide an appropriate means for specifying orientation. Instead, quaternions are used for this purpose. Since a quaternion is a four-dimensional vector, and a MARG sensor produces nine signals, this data processing problem is "overspecified". This fact can be used to discriminate against sensor noise and to reduce the effects of linear acceleration on measurement of the gravity vector by accelerometers. Detailed computer simulation studies and the results of preliminary experiments with a prototype body tracking system confirm the effectiveness of the quaternion body-tracking filter.*

## 1. Introduction

Since early times, the gravitational field of the Earth has been used to define the local vertical or "down" direction. Devices such as plumb bobs were used to measure the slope of Egyptian pyramids and many other early buildings and walls. With the advent of sailing ships (if not earlier), the notion of "pitch" and "roll" angles as a measure of deviation from the vertical was introduced. Much later, perhaps a thousand years ago or so, the compass was invented as a means of measuring a third orientation angle usually called “heading”. In the nineteenth century these angles were named “Euler” angles and their mathematical description was formalized (McGhee at al., 2000).

As sailing ships grew in size and capability, long range navigation at sea, out of sight of land, became very important. The compass was a critical invention in enabling long distance sailing, with Columbus’ voyages to the “New World” being the most widely known early example. Various forms of sextants were also in use in ancient times to determine latitude from measurement of elevation angles to known stars. Such measurements required correction for ship pitch and roll angles to be effective. This was done with a plumb bob, bubble level, or similar device. Removal of pitch and roll effects on compasses on shipboard was usually achieved by floating the compass needle (or “heading rose”) on a liquid which remained more or less level relative to the horizon during ship pitching and rolling under wave and wind action. With the introduction of compasses to aircraft navigation, this approach no longer worked and instead spinning *vertical gyros* were used to maintain an “artificial horizon” during sustained aircraft maneuvers. In such applications, three-axis magnetometers are sometimes used to measure the Earth’s magnetic field, and heading then computed from values for pitch and roll angles obtained from sensors attached to the vertical gyro (Frey, 1996). A similar approach is currently used in miniaturized electronic compasses intended for marine navigation applications (Precision Navigation, 2000).

For real-time human limb segment tracking, most current methods use active sources of some sort to track either angles or the position of reference points on limbs or joints (Meyer et al., 1992; Molet et al., 1999). While this has worked well for some applications, such approaches typically either seriously encumber the subject, or work only over limited ranges, or both. However, in the case of head tracking, recent advances in sensor technology and small computers have made it possible to achieve effective sourceless tracking using only the Earth’s gravitational and magnetic fields as references for determination of orientation, analogous to the ship and aircraft systems described above. Head trackers of this type are now commercially available (Foxlin, 1994), and typically use some variant of MARG (Magnetic field, Angular Rate, and Gravity) sensors to determine values for head Euler angles. Full details of a similar system developed for small unmanned submarine navigation can be found in (Yun et al., 1999). The purpose of the present paper is to describe and evaluate alternative algorithms needed to extend sourceless tracking technology from head motion to full body motion. As will be seen, major changes in MARG sensor data processing techniques are needed if robust and cost-effective body tracking is to be achieved.

## 2. Quaternion Basics

A fundamental problem with full body tracking using Euler angles arises from the fact that when a rigid body (or limb segment) is in a vertical orientation, heading and roll (bank) Euler angles are undefined, and cannot be uniquely determined. Even more seriously, the body rate to Euler angle rate transformation matrix (needed to derive Euler angle rates from body-fixed angular rate sensors) is singular for this orientation (McGhee et al., 2000). Fortunately, quaternions do not suffer from this problem since they express rigid body orientation in terms of a single rotation about an inclined axis. A common way of expressing such an “angle-axis” pair in terms of a unit quaternion is:

$$q = \cos(\Theta / 2) + u \sin(\Theta / 2) \tag{1}$$

where $\Theta$ is the rotation angle, and $u$ is a unit three-dimensional “rotation axis” vector (McGhee et al., 2000). In this form, a unit quaternion looks very much like the *polar* form of a unit complex number:

$$z = \cos(\Theta) + i \sin(\Theta) = e^{i\Theta} \tag{2}$$

where $i$ is a “flag” designating the second (“imaginary”) element of a two-dimensional vector. Indeed, it is well known that a unit complex number accomplishes planar rotation of two-dimensional vectors under complex multiplication. That is, if

$$z_1 = x_1 + iy_1 = r_1\ e^{i\,\Theta_1} \tag{3}$$

and

$$z_2 = e^{i\ \Theta_2} \tag{4}$$

then

$$z_1 z_2 = z_2 z_1 = r_1 e^{i(\Theta_1 + \Theta_2)} \tag{5}$$

For quaternion rotation of three-dimensional vectors, the corresponding relationship is:

$$v_2 = q \otimes v_1 \otimes q^{-1} \tag{6}$$

where $v_1$ is any three-dimensional vector (quaternion with 0 for first component) and $\otimes$ denotes the quaternion product (McGhee et al., 2000).

There are several equivalent ways to define the quaternion product (McGhee et al., 2000). The original approach, used by Hamilton, the discoverer of quaternions, was to view a quaternion as a four-dimensional generalization of a complex number, written as

$$q = w + u\ s \tag{7}$$

where $w$ is the “real” part and $s$ is the magnitude of the “vector” part. More precisely, what this equation really means is:

$$q = (w\ 0\ 0\ 0) + (0\ x\ y\ z) = (w\ x\ y\ z) \tag{8}$$

where “+” is a vector sum and $u$ is the unit vector

$$u = (0\ u_z\ u_y\ u_z) \tag{9}$$

Since $u$ has only three non-zero components, it is also possible to describe it using the "flag" notation:

$$u = i\,u_x + j\,u_y + k\,u_z \tag{10}$$

By analogy to complex numbers, Hamilton defined a *flag algebra* as:

$$i \otimes i = j \otimes j = k \otimes k = -1 = (-1 \;\; 0 \;\; 0 \;\; 0) \tag{11}$$

and

$$i \otimes j \otimes k = (-1 \;\; 0 \;\; 0 \;\; 0) \tag{12}$$

From these two definitions, it follows that

$$i \otimes j = k = -j \otimes i, \quad k \otimes i = j = -i \otimes k, \quad j \otimes k = i = -k \otimes j \tag{13}$$

The quaternion product is thus seen to have some of the features of the two-dimensional "complex" product, and some of the features of the three-dimensional vector "cross product" (McGhee et al., 2000). Analogous to the case with complex numbers and three-dimensional vectors, flag algebra allows scalar algebra and scalar calculus to be applied to quaternion analysis.

Again by analogy to complex numbers, the *conjugate* of a quaternion, denoted as $q^*$, is obtained by merely negating its vector part. That is, if $q$ is written in the form of Eq. (8), then

$$q^* = (w \;\; -x \;\; -y \;\; -z) \tag{14}$$

It is a straightforward exercise in quaternion algebra (using Eq. (11) and (13)) to show that

$$q \otimes q^* = q^* \otimes q = w^2 + x^2 + y^2 + z^2 = |q|^2 \tag{15}$$

From this result, it is evident that Eq. (1) does in fact describe any unit quaternion. It is also clear from this relation that the inverse of any unit quaternion is just its conjugate. Evidently, for an arbitrary quaternion,

$$q^{-1} = \frac{q^*}{q \otimes q^*} \tag{16}$$

These definitions allow the computation of all terms appearing in Eq. (6), the basic relation for transforming points attached to a rigid body to the corresponding points in world coordinates. It is noteworthy that this approach is much less computationally demanding than the more common "rotation matrix" approach typically used in computer graphics for such transformations (McGhee et al., 2000).

## 3. Quaternion Filter

While all possible Euler angle sets are singular (non-unique) in some orientation, and body rate to Euler rate transformations are computationally expensive since they require vector-matrix products involving many trigonometric functions, determination of quaternion rates from body rates is free of both of these problems (McGhee et al., 2000). Specifically, if the reserved symbols *p*, *q*, and *r* are used for roll rate, pitch rate, and yaw rate respectively, then (Cooke et al., 1992; Kuipers 1998):

$$\dot{q} = \frac{1}{2} q \otimes (0 \ p \ q \ r) \tag{17}$$

In understanding this equation, it is important to realize that the symbol *q* has been overloaded, standing both for a quaternion and for pitch rate. Since both usages are standard, the authors have elected to write the equation in this form, trusting that any potential ambiguities will be resolved by context.

If an extremely accurate rate sensor is available (such as a ring laser gyro for example), then orientation can be determined by simply integrating this rate (Lawrence, 1998). However, such sensors are large, heavy, and expensive, and not at all practical for human body segment tracking. Instead, micromachined "vibrating beam" sensors are more suitable for this purpose (Teegarden et al., 1998). While this type of sensor is inexpensive, lightweight, rugged, very small in physical dimensions, and requires negligible electrical power, its accuracy is such that errors resulting from integration of Eq. (17) become unacceptable after only a few seconds. This being the case, some form of "drift correction" is required to obtain accurate results from integrating this equation. Figure 1 below shows one way that this can be done (Bachmann et al., 1999).

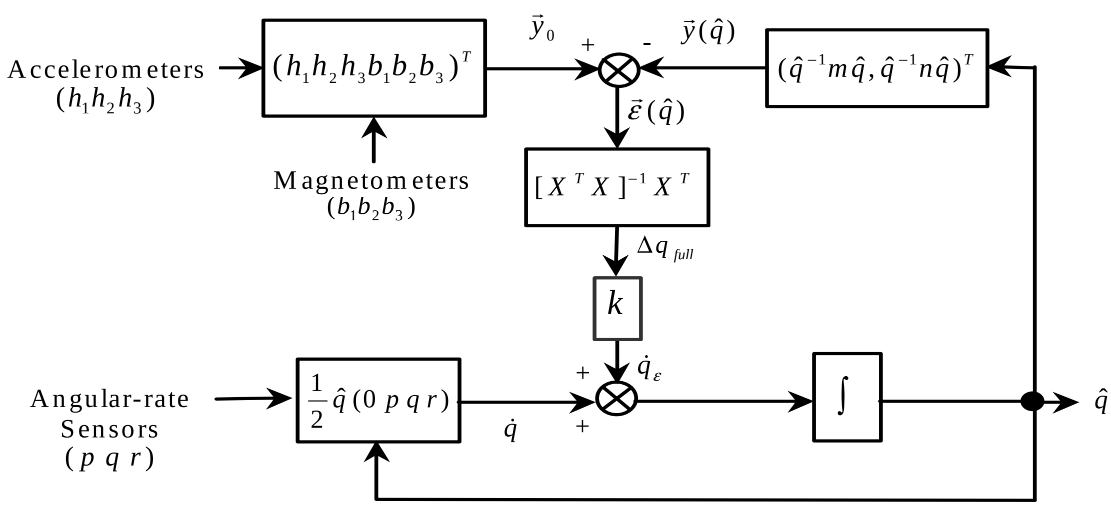


**Figure 1: Quaternion-Based Orientation Filter**

As can be seen from this figure, drift correction is provided by the accelerometer and magnetometer components of a MARG sensor. Specifically, the vector *h* is a unit vector pointing in the direction of the total sensed acceleration (gravity plus linear acceleration), while the vector *b* is a unit vector aligned with the total magnetic field vector (earth field plus local disturbances). The vector $\vec{y}_0$ is thus a six dimensional vector composed of these two unit vectors. The quaternion $\hat{q}$ is the estimated orientation quaternion for the body being tracked, so $\vec{y}(\hat{q})$ is a *computed measurement* vector determined from $\hat{q}$. In order to make this computation, it is necessary to use the known values $m = (0\ 0\ 0\ 1)$ for the gravity unit vector and $n = (0\ n_x\ n_y\ n_z)$ for the local magnetic field vector. With this understanding, it is evident that the *modeling error* vector, $\varepsilon(\hat{q})$, represents the difference between what the sensors measure and what the quaternion filter predicts should be measured.

Further examination of Figure 1 shows that the quaternion used to compute $\vec{y}(\hat{q})$ is the inverse of the orientation quaternion. This is because $\hat{q}$ transforms points in body (sensor) coordinates to the corresponding points in world coordinates whereas the reverse transformation is needed to compute $\vec{\varepsilon}(\hat{q})$ in sensor coordinates (McGhee et al., 2000). At this point in understanding this filter, it is important to recognize that while $\vec{\varepsilon}(\hat{q})$ is a six-dimensional vector, the *drift correction* signal, $\dot{q}_e$, is of dimension four. This means that a 4 x 6 matrix or some other transformation is needed to compute a value for the drift correction component of $\dot{\hat{q}}$ from the modeling error vector. There is a vast body of literature on this type of problem generally referred to as *Kalman filter theory*, or more generally, *optimal least-squares estimation theory* (Brown & Hwang, 1997). In this paper, a simpler approach called *non-linear regression analysis* will be used. As will be seen in the following section of this paper, this method explains the relation

$$\dot{q}_e = k[X^T X]^{-1} X^T\ \vec{\varepsilon}(\hat{q}) \tag{18}$$

shown in Figure 1.

## 4. Non-linear Regression and Gauss-Newton Iteration

Suppose that a vector *dependent variable*, y, depends on a vector *independent variable, x*. The general form of such a relationship is

$$y = f(x) \tag{19}$$

Now let $y_0$ denote a *measured value* for $y$ obtained in some type of experimental setting. In general, any real physical measurement will be to some degree corrupted by random noise. When such noise is additive (the most common assumption) (Brown & Hwang, 1997), $y_0$ takes the form

$$y_0 = f(x) + \eta \tag{20}$$

where $\eta$ is the (unknown) *measurement noise* vector. The fundamental problem of non-linear regression analysis is to obtain a "best estimate" for an unknown $x$ from a given function $f$ and a known (measured) value for $y_0$ (McGhee, 1967; Everitt, 1987).

In regression analysis, it is required that the dimension of $y$ be greater than the dimension of $x$. This means that there is in general no value, $x = \hat{x}$, such that $f(\hat{x}) = y_0$. That is, to borrow terminology from linear algebra, there are "fewer unknowns than equations" when $y_0$ has more components than $x$. Problems of this type are said to be "overspecified" (Strang, 1988). In such cases, what is most often done is to define an *error* vector, $\vec{\varepsilon}$, as a column vector of *M* rows given by:

$$\vec{\varepsilon}(x) = y_0 - f(x) \tag{21}$$

and to then try to find an $x = \hat{x}$ that minimizes the scalar *squared error criterion function* (McGhee, 1967):

$$\varphi(x) = \vec{\varepsilon}(x)^T \vec{\varepsilon}(x) \tag{22}$$

The minimizing value for $\varphi$, namely $x = \hat{x}$, is called the *least squares estimate* of the (unknown) true value for $x$.

Minimization of a non-linear function such as $\varphi(x)$ is a basic problem, which has received much attention in mathematics for centuries. The widespread availability of digital computers, beginning about forty years ago, allowed much more complex minimization problems to be solved, and spurred a renewed interest in the mathematical underpinnings of optimization problems in general. One approach, which has proved to be effective for many regression problems, is *Gauss-Newton* iteration (Hartley, 1961; McGhee, 1963). In this technique, the *M* row vector function $f(x)$ is *linearized* about a given value, $x = x_0$, by using the first two terms in its Taylor series expansion, namely:

$$f(x_0 + \Delta x) = f(x_0) + X\Delta x + O(\Delta x^2) \tag{23}$$

where $x_0$ and $\Delta x$ are column vectors of *N* rows, *N* < *M*, and $X$ is the *M* x *N* matrix of partial derivatives:

$$X_{ij} = \frac{\partial f_i}{\partial x_j} \tag{24}$$

In utilizing Eq. (23), it is important to recognize that $X$ is evaluated at $x = x_0$, and is therefore a constant matrix relative to changes in $x$ about that value. Specifically, in what follows,

$$\frac{dX}{dx} = \frac{dX}{d\Delta x} = 0 \tag{25}$$

Using only the linear part of Eq. (23), the error vector, $\vec{\varepsilon}$, can be approximated as:

$$\vec{\varepsilon}(x_0 + \Delta x) = y_0 - f(x_0) - X\Delta x = \vec{\varepsilon}_0 - X\Delta x \tag{26}$$

From the inverse law of transposed products (Strang, 1988), it follows that:

$$\vec{\varepsilon}(x_0 + \Delta x)^T = \vec{\varepsilon}_0^T - \Delta x^T X^T \tag{27}$$

Thus, from Eq. (22), the criterion function, $\varphi(x)$, is approximated by:

$$\varphi(x) = \vec{\varepsilon}_0^T \vec{\varepsilon}_0 - \vec{\varepsilon}_0^T X\Delta x - \Delta x^T X^T \vec{\varepsilon}_0 + \Delta x^T X^T X\Delta x \tag{28}$$

which (providing $X$ is of full rank) is a positive definite quadratic form in $\Delta x$ (Strang 1988; Cormen et al. 1994). Noting that every term in this equation is a scalar, and again using the inverse law of transposed matrices, it follows that

$$\vec{\varepsilon}_0^T X\Delta x = \Delta x^T X^T \vec{\varepsilon}_0 \tag{29}$$

so Eq. (28) can be simplified to:

$$\varphi(x) = \vec{\varepsilon}_0{}^T \vec{\varepsilon}_0 - 2\Delta x^T X^T \vec{\varepsilon}_0 + \Delta x^T X^T X\Delta x \tag{30}$$

From vector calculus (Rust & Burrus, 1972), using this expression, and Eq. (25), the *gradient* (vector derivative) of $\varphi$ is given by:

$$\frac{d\varphi}{dx} = -2X^T \vec{\varepsilon}_0 + 2X^T X\Delta x \tag{31}$$

When $\varphi(x)$ is positive definite, the unique minimum of Eq. (30) is found by equating the above gradient to 0 with the result:

$$\Delta x = [X^T X]^{-1} X^T \vec{\varepsilon}_0 \tag{32}$$

This equation defines Gauss-Newton iteration and explains Eq. (18), and the corresponding block of Figure 1, except for the scalar feedback gain factor, $k$. This factor relates to the stability and accuracy of the quaternion filter, and will be the subject of further discussion later in this paper.

All of the above analysis assumes that the neglected $O(\Delta x^2)$ term in Eq. (23) is not important. This is often not the case, so in many problems it is necessary to apply Eq. (32) iteratively. This issue is investigated for the case of orientation quaternion estimation in a later section this paper.

## 5. Gauss-Newton Iteration for Quaternion Filter

Appendix A derives the $X$ matrix of Figure 1 for an arbitrary non-zero quaternion, $q$, and also shows that multiplying any such quaternion by a non-zero scalar has no effect on the computed measurement vector, $y(q)$, shown in Figure 1. Unfortunately, this latter fact means that $\hat{q}$ is not unique. This has the further consequence that $X$ is not of full rank, and therefore the *regression matrix*

$$S = X^T X \tag{33}$$

appearing in Eq. (18) and (32) is *singular* (Strang, 1988). This means that $S$ has no inverse, and therefore this $X$ matrix cannot be used in Gauss-Newton iteration. Numerical experiments show that this is indeed the case. While this might at first seem to be extremely serious with respect to the correct functioning of the quaternion filter of Figure 1, this is not so. In fact, as described below, there are at least two distinct ways of dealing with the singularity of $S$.

The most straightforward way to resolve the non-uniqueness problem for $\hat{q}$ is to restrict it to be a unit quaternion. Specifically, if the output of the integrator block on Figure 1 is labeled $\tilde{q}$, then $\tilde{q}$ can be *normalized* to a unit quaternion by adding an extra block that accomplishes the calculation:

$$\hat{q} = \frac{\tilde{q}}{|\tilde{q}|} \tag{34}$$

Somewhat surprisingly, this constraint also permits computationally significant improvements to the calculation of the $X$ matrix. Specifically, since the inverse of a unit quaternion is just its conjugate, Eq. (A-5) simplifies to (Henault, 1997):

$$\frac{\partial q^{-1}}{\partial q_0} = 1 \tag{35}$$

$$\frac{\partial q^{-1}}{\partial q_1} = -i \tag{36}$$

$$\frac{\partial q^{-1}}{\partial q_2} = -j \tag{37}$$

and

$$\frac{\partial q^{-1}}{\partial q_3} = -k \tag{38}$$

Eq. (A-7) is likewise simplified by this substitution. In particular, using these results, from the product rule of differential calculus:

$$\frac{\partial y}{\partial q_0} = \left(m \otimes q + q^{-1} \otimes m,\ n \otimes q + q^{-1} \otimes n\right)^T \tag{39}$$

$$\frac{\partial y}{\partial q_1} = \left(-i \otimes m \otimes q + q^{-1} \otimes m \otimes i,\ -i \otimes n \otimes q + q^{-1} \otimes n \otimes i\right)^T \tag{40}$$

$$\frac{\partial y}{\partial q_2} = \left(-j \otimes m \otimes q + q^{-1} \otimes m \otimes j,\ -j \otimes n \otimes q + q^{-1} \otimes n \otimes j\right)^T \tag{41}$$

$$\frac{\partial y}{\partial q_3} = \left(-k \otimes m \otimes q + q^{-1} \otimes m \otimes k,\ -k \otimes n \otimes q + q^{-1} \otimes n \otimes k\right)^T \tag{42}$$

In all of these expressions, it is to be understood that only the vector part of each triple quaternion product is used, and that the comma denotes concatenation. Thus, each of the above expressions constitutes one 6 x 1 column of the $X$ matrix. While these equations yield a numerically different $X$ matrix from that of Appendix A, simulation experiments show that, when $\hat{q}$ is normalized to a unit quaternion on every computation cycle, then the associated matrix is not singular and Gauss-Newton iteration using these relations succeeds.

The second alternative to the computation of $\hat{q}$ results from noting that if

$$\hat{q}_{new} = \hat{q}_{old} + \Delta q_{full} \tag{43}$$

and if both $\hat{q}_{new}$ and $\hat{q}_{old}$ are unit quaternions, then any small $\Delta q_{full}$ must be orthogonal to $\hat{q}$. That is, the only way to alter a unit vector while maintaining unit length is to rotate it, and for small rotations $\Delta q$ must therefore be tangent to the unit four-dimensional sphere defined by equating Eq. (15) to 1. From the Orthogonal Quaternion Theorem of Appendix B, this means that:

$$\Delta q = \hat{q} \otimes \left(0\, v_1\, v_2\, v_3\right) \tag{44}$$

With this constraint, linearization of the *expected measurement* vector, y(q), in Figure 1, yields

$$y(q+\Delta q) = y(q) + X\Delta q = y(q) + X\left(q \otimes (0\, v_1\, v_2\, v_3)\right)^T \tag{45}$$

and consequently:

$$\frac{\partial y}{\partial v_1} = X\left(q \otimes (0\ 1\ 0\ 0)\right) = X\left(q \otimes i\right)^T \tag{46}$$

$$\frac{\partial y}{\partial v_2} = X\left(q \otimes (0\ 0\ 1\ 0)\right) = X\left(q \otimes j\right)^T \tag{47}$$

and

$$\frac{\partial y}{\partial v_3} = X\left(q \otimes (0\ 0\ 0\ 1)\right) = X\left(q \otimes k\right)^T \tag{48}$$

From Eq. (44), it is evident that when Gauss-Newton iteration is applied to unit quaternions, it is sufficient to solve for only three unknowns rather than four as in the methods for estimation of $\Delta q_{full}$ considered until now. That is, if $X$ is the 6 x 3 matrix

$$X_v = \left[ \frac{\partial y}{\partial v_1} \middle| \frac{\partial y}{\partial v_2} \middle| \frac{\partial y}{\partial v_3} \right] \tag{49}$$

then,

$$\Delta v_{full} = \left[X_v{}^T X_v\right]^{-1} X_v \vec{\varepsilon}(\hat{q}) \tag{50}$$

and

$$\Delta q_{full} = \hat{q} \otimes \left(0,\ \Delta v_{full}\right) \tag{51}$$

Simulation experiments show that this result functions correctly in Gauss-Newton iteration using either the $X$ matrix of Appendix A or the modified $X$ matrix defined by Eq. (39) – (42).

When both of the above improvements are incorporated into the Gauss-Newton algorithm, simulation results are the same as those obtained from either one applied alone. Since Eq. (39) – (42) notably simplify the computation of the $X$ matrix, and Eq. (50) involves a 3 x 3 matrix inversion rather than the 4 x 4 matrix inversion of the basic algorithm, a considerable reduction in the time required for execution of one cycle of Gauss-Newton iteration results from use of a combined algorithm. In this regard, it is particularly important that it is known that the best algorithms for matrix inversion are of $O(n^3)$ complexity (Cormen et al., 1994).

As a final observation on uniqueness, while any of the above modifications to the results of Appendix A solves the problem of a singular regression matrix, from Eq. (A-2), it is evident that $-\hat{q}$ produces the same computed measurement vector as $\hat{q}$. This means that if the initial error in $\hat{q}$ is very large, then Gauss-Newton iteration can produce either of two answers, one with a negative real part, the other with a positive real part. While this is of no consequence to body tracking, it does matter in some applications. One such example is provided by rigid body dynamics (McGhee et al., 2000). In such cases, it is a simple matter to achieve uniqueness by transforming the result of any quaternion calculation to *positive real form* by simply negating any result with a negative real part.

## 6. Convergence and Accuracy of Orientation Quaternion Estimation by Gauss-Newton Iteration

The convergence of Gauss-Newton iteration can be investigated from either a local or global perspective. Conditions for local convergence are known, and are derived by writing the Taylor series for the criterion function, $\varphi(q)$, through the second derivative term, and then computing the eigenvalues of a specific matrix involving the regression matrix, $S$ (McGhee, 1963; Bekey & McGhee, 1964). If local convergence conditions are satisfied at one or more points inside a bounded search volume, then an algorithm exists which returns, with probability arbitrarily close to one, the value of $q$ that produces the true minimum of $\varphi(q)$ within the search volume (McGhee, 1967).

By restricting $\hat{q}$ to be a unit quaternion, the search volume is confined to the surface of a unit four-dimensional sphere. This fact guarantees global convergence to a true minimum value of $\varphi(q)$, providing that local convergence conditions are satisfied. Since it is very difficult to establish by analytic means that this is the case for all unit quaternions and all possible levels of measurement noise, this question has been studied by computer simulation. Specifically, several hundred simulation trials were conducted in which a random unit quaternion called "$q_{true}$" was generated along with another random (uncorrelated) unit quaternion called "$q_{start}$". Using noiseless synthetic data generated from $q_{true}$ by means of Eq. (A-6), and starting Gauss-Newton iteration at $q_{start}$, no failures to converge were observed after ten cycles of iteration, although as expected, convergence to $-q_{true}$ was found to be just as likely as convergence to $q_{true}$. Evidently, Gauss-Newton iteration is very robust when applied to the orientation quaternion estimation problem. Interested readers are invited to explore this issue further by means of additional simulation trials using the test functions t1 through t3 included in the Lisp code available at http://npsnet.org/~bachmann/research.htm

The above discussion relates to filter initialization only since any useful filter must have the property that previous and updated values for $\hat{q}$ differ by only a small amount. That is, the very nature of "tracking" means that a reasonably good estimate for the current $q_{true}$ is available at all times following initialization. To test tracking properties of Gauss-Newton iteration, another simulation was conducted in which $q_{start}$ was produced by adding uniformly distributed noise with a maximum value of +/- 0.1 to each component of $q_{true}$. This is felt to be a rather severe test of the tracking capabilities of Gauss-Newton iteration since it corresponds to tracking errors of the order of 11.5% for unit quaternions. To see that this is so, let

$$q_{start} = q_{true} + \eta \tag{52}$$

and let $\gamma$ be a random variable uniformly distributed in the interval (-1, 1). Then, the variance, $\sigma_\gamma^{\ 2}$, of $\gamma$ is given by (Levine, 1971),

$$\sigma_\gamma^{\ 2} = \int_{-1}^{1} \frac{1}{2}\gamma^2 \, d\gamma = \frac{1}{3} \tag{53}$$

From this result, if $\eta_{\max}$ is the maximum absolute error in any component of $q_{start}$ (equal to .1 in the above discussion), then since each of the four components of $\eta$ is independently generated, it follows that the *expected root mean square error* in $q_{start}$ is given by:

$$\sigma_\eta = \sqrt{4\left(\frac{1}{3}\right)\eta_{\max}^{\ 2}} = \sqrt{\frac{4}{300}} = .115 \tag{54}$$

That is, the *rms* (root mean square) length of $\eta$ is this number, which is 11.5% of the length of a unit quaternion.

After generating $q_{true}$ and $q_{start}$, a six-dimensional vector of noiseless synthetic data was again generated using Eq. (A-6). Following this step, six-dimensional uniformly distributed noise in the range (-max-noise, max-noise) was added to this data. That is, the *simulated measurement* was computed as:

$$y_0 = y(q_{true}) + \delta \tag{55}$$

where each component of $\delta$ is a sample of uniformly distributed noise in the above interval. By analogy to Eq. (54), it follows that:

$$\sigma_\delta = \sqrt{6\left(\frac{1}{3}\right)\delta_{\max}^{\ 2}} = 1.414\,\delta_{\max} \tag{56}$$

That is, the rms length of $\delta$ is approximately 40% more than the maximum absolute error in any of its six components. Using this type of synthetic data, a series of simulation experiments was carried out in which the rms accuracy of Gauss-Newton iteration was evaluated as a function of max-noise and the number of cycles of iteration within each experiment. The results of this study are summarized in Table 1. Each cell of this table is associated with the length of the error in $\hat{q}$ averaged over one hundred random trials. New data was generated for each cell, so this table shows both systematic tendencies and random (sampling) fluctuations. The following paragraphs discuss the significance of the tabulated results.

| Max. Noise per Component | Number of Gauss-Newton Iteration Cycles | | |
|---|---|---|---|
| | 1 | 2 | 3 |
| 0.0 | 0.0066782855 | 3.1667924e-5 | 9.276619e-8 |
| 0.001 | 0.006650507 | 8.304288e-4 | 8.1245136e-4 |
| 0.01 | 0.011104382 | 0.008134228 | 0.007868233 |
| 0.1 | 0.07969765 | 0.08627058 | 0.08296164 |

**Table 1: Observed RMS Error in Estimated Orientation Quaternion as a Function of Sensor Noise Level and Number of Cycles of Gauss-Newton Iteration**

Considering first the top row of Table 1, it can be seen that no failures to converge occurred in any of the three sets of one hundred experiments associated with each entry in this row. Moreover, $\hat{q}$ never converged to $-q_{true}$ as was observed often in the initialization experiments described at the beginning of this section of this paper. This is because initialization involves completely random values for $q_{start}$, while all of the experiments of Table I use a $q_{start}$ with a maximum error of +/- 0.1 in each component. This means that $-q_{true}$ is not in the "domain of attraction" of $q_{start}$ for these trials. Further examination of this row shows that, during tracking, three cycles of Gauss-Newton with noiseless data results in estimation errors which are in the level of round-off errors. This is in contrast to initialization experiments in which it was found, as reported above, that somewhat more cycles are needed to achieve convergence when $q_{start}$ is completely random.

Turning to the second row of Table I, it can be seen that two cycles of Gauss-Newton iteration are sufficient when the maximum absolute value for the noise on each data component is equal to .001. In addition, the length of the vector error in $\hat{q}$ is seen to be approximately 80% of the maximum noise per component. Examining the third row of the table shows that these two features persist when the maximum noise level is increased to .01. When the sensor maximum noise is increased to .1 (an unreasonably large value), the last row of Table I reveals an apparently anomalous behavior in that more Gauss-Newton iteration cycles result in *less* accuracy. However, as confirmed by additional experiments not reported here, this effect is just the result of statistical fluctuations due to the independent trials associated with every entry in this table. The more important conclusion from this row is that, with uniformly distributed noise on synthetic data samples, even at such unrealistically large noise levels, the average length of the vector error in $\hat{q}$ is seen to remain at approximately 80% of the maximum data component noise level.

Lisp code for the simulation study reported in Table I is available at http://npsnet.org/~bachmann/research.htm, and the interested reader is invited to use the functions t4 through t15 defined in this code to confirm or extend the results reported here. However, the authors believe that the results of this table are sufficient to show that Gauss-Newton iteration provides both the stability and accuracy needed for implementation of the drift correction feedback loop shown in Figure 1. The next section of this paper presents a modification to Gauss-Newton iteration which could be applied when errors in magnetometer data are either larger or smaller than those in accelerometer data, and also discusses criteria and methods for choosing the scalar gain factor, *k*, when Gauss-Newton iteration is combined with integration of $\dot{q}$ values obtained from angular rate sensors.

## 7. Filter Tuning: Weighted Least Squares Regression and Complementary Filtering

Referring again to Figure 1, the possibility exists of putting greater or less reliance on magnetometer data in comparison to accelerometer data. This could come about because one or the other of these signals could prove to be less accurate (or noisier) than the other. This can be achieved by merely redefining the error vector, $\varepsilon$, as:

$$\varepsilon(\hat{q}) = \begin{bmatrix} y_{0_1} - y(\hat{q})_1 \\ y_{0_2} - y(\hat{q})_2 \\ y_{0_3} - y(\hat{q})_3 \\ \rho\left(y_{0_4} - y(\hat{q})_4\right) \\ \rho\left(y_{0_5} - y(\hat{q})_5\right) \\ \rho\left(y_{0_6} - y(\hat{q})_6\right) \end{bmatrix} \tag{57}$$

Evidently, $\rho > 1$ emphasizes magnetometer data, while $0 < \rho < 1$ puts greater weight on accelerometer data. Clearly, this change also alters the $X$ matrix, simply by multiplying the last three elements of each column by $\rho^2$. If a detailed statistical model is available for magnetometer and accelerometer errors for a particular experimental setting then, at least conceptually, the best value for $\rho$ could be obtained either from Kalman filter theory (Brown & Hwang, 1997) or from some other statistical theory such as “maximum likelihood” parameter estimation (Levine, 1971). However, the authors are inclined to believe that this will usually be impractical for human body tracking applications, and that it is probably more productive to think of $\rho$ as a “tunable” parameter adjusted by “eyeball optimization” in a given situation.

All of the analysis and simulation up to this point in this paper has dealt only with the application of Gauss-Newton iteration to *static* problems. That is, it has been assumed that only one measurement vector is available, and the Gauss-Newton procedure is applied iteratively to find $\Delta q_{full}$ as shown in Figure 1. While this kind of computation may be useful in some applications, body tracking is a *dynamic* problem in which estimation of the orientation quaternion must proceed in real-time, and in parallel with the acquisition of new data during the course of limb segment and body motion. As mentioned previously, there is a large body of knowledge dealing with such problems, ordinarily called *filter theory* (Brown & Hwang, 1997). This theory provides a means for analyzing the effects of the other tunable parameter in the quaternion orientation filter of Figure 1, namely the *feedback gain* factor, *k*.

The facts that Table I shows that rms estimated orientation quaternion errors are linearly related to rms sensor noise level, and that only one cycle of Gauss-Newton iteration may be sufficient in practical orientation tracking, imply that a *linearization* of Figure 1 is possible for purposes of stability analysis and investigation of the effects of the value of the feedback gain, *k*. Such a linearization is based on the recognition that, during tracking, even on the first Gauss-Newton iteration, it is a good approximation to assume that

$$\Delta q_{full} = q_{true} - \hat{q} \tag{58}$$

Figure 2 below shows a linearized version of Figure 1 based on this assumption.

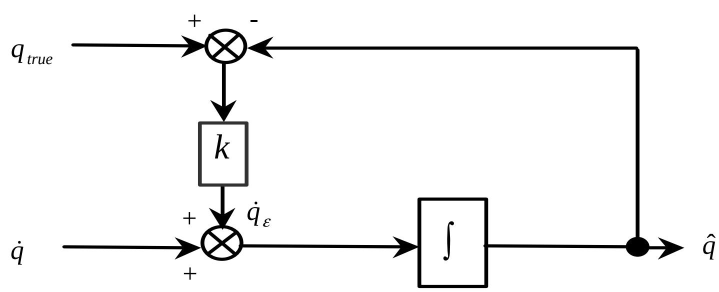


**Figure 2: Linearized Orientation Quaternion Estimation Filter**

This filter has the form of a *complementary* filter (Brown & Hwang, 1997) in which the integral of $\dot{q}$, which is accurate for short periods of time, is "complemented" by the integral of the *drift correction derivative*, $\dot{q}_{\varepsilon}$, which is dependable only when averaged over longer periods of time to counteract the confounding effects of linear acceleration on the measurement of gravity and of stray magnetic fields on the determination of heading. A key feature of complementary filters is the idea of a *crossover frequency* below which signals from one type of sensor are given greater weighting, and above which signals from another type of sensor are favored. From linear system theory (McGhee at al., 1995; Brown, 1997), the crossover frequency for Figure 2 is given by

$$f_c = \frac{k}{2\pi} Hz \tag{59}$$

The meaning of this result is that below this frequency accelerometer and magnetometer signals are given greater emphasis, while above this frequency, rate sensor signals are more trusted. While it is possible to optimize *k* if full statistical information about sensor signal and noise characteristics is available, the authors doubt that this will often be the case, and believe instead that *k* is a parameter which, like the *magnetometer emphasis factor*, $\rho$, should be "tuned by eyeball" in a given experimental setting. Experience with this approach to date suggests that $f_c$ should generally be somewhat less than the lowest significant frequency of linear acceleration resulting from limb segment motion. A more detailed discussion of guidelines for choosing a value for *k*, along with preliminary experimental results of human arm tracking can be found in (Bachmann, 2000). In these experiments, for the MARG sensor used, and for the type of motion tracked, values of *k* somewhere in the range $1.0 < k < 4.0$ were found to be appropriate. Much more research on this issue in a variety of experimental contexts is still needed.

As a final remark, it should be recognized that Figure 1 and Figure 2 represent continuous time or *analog* realizations of orientation quaternion tracking. While this would be possible if the $X$ matrix were constant, in fact it is not and must be reevaluated on every cycle of Gauss-Newton iteration. This means that only a discrete time or *digital* filter is possible. This represents no problem if the integration in these figures is simply approximated by a discrete sum, providing that the update cycle time is short enough. The fact that Figure 2 is linear allows this issue to be treated analytically (Bachmann, 2000), but such analysis is beyond the scope of this paper.

## 8. Summary and Conclusions

While sourceless tracking of human head motion using only the gravitational and magnetic fields of the Earth as orientation references has been accomplished and commercialized (Foxlin, 1994), there has been, until recently (Bachmann, 2000), no corresponding success in whole body limb segment tracking. The authors of this paper believe that success in such an endeavor requires not only better MARG sensor packages than are currently commercially available, but also a completely different approach to sensor data processing than has been used for head tracking and related ship and aircraft navigation systems. The primary purpose of the present paper is to present an efficient and robust algorithm for sourceless real-time tracking and subsequent display of human limb motion, which is free of the singularity problems and computational complexity of prior algorithms based on Euler angles or anatomical joint angles (Semwai et al., 1998; Molet et al., 1999; Bachmann, 2000).

The algorithm which has been discovered in the course of this research relies on the Orthogonal Quaternion Theorem, which is believed to be a new result. This theorem both resolves the singularity problem of Gauss-Newton iteration applied to orientation quaternion tracking, and reduces the size of the associated regression matrix from 4 x 4 to 3 x 3. Since inversion of this matrix is probably the most time consuming part of Gauss-Newton iteration, and matrix inversion is of $O(n^3)$ complexity, where *n* is the size of the matrix, the computational advantages arising from the application of this theorem are substantial, and are especially important when simultaneously tracking a large number of human limb segments.

An important feature of the algorithm we have developed is that it contains two scalar gain factors that allow “tuning” of the filter to fit a particular tracking situation. Preliminary guidelines for choosing values for these parameters have been provided and are included in (Bachmann, 2000) However, it is believed that final selection of gains is best accomplished by adjustment during the course of an experiment, analogous to the way the controls of a radio are adjusted by a listener to get the desired tone quality, speaker balance, etc. We think that this is a new idea with respect to sourceless tracking, and of sufficient importance that we have decided to name our procedure the “Tuneable Quaternion Tracker” (TQT) algorithm.

The TQT algorithm is designed to function with nine-axis MARG sensors as described in the body of this paper and illustrated in Figure 1. However, it is important to recognize that in static problems (or in situations where angular rates and linear accelerations are sufficiently low) the angular rate sensing and integration part of this algorithm may not be needed. That is, another way of looking at the TQT algorithm is that the angular rate portion of the algorithm is needed only to “quicken” the response of the filter to compensate for the lag in Gauss-Newton estimation introduced by the scalar gain $k$ in the drift correction feedback loop. If the actual motion being tracked is sufficiently slow, such quickening may not be needed. In such cases, rate sensing will not be required and the MARG sensor can be simplified to a six-axis device.

As a final remark, we are aware that this paper does not present any details regarding the actual implementation and tracking of human limb motions in real time. In fact, we have only preliminary results in this area (Bachmann et al., 1999), but an intensive effort in sensor improvement and in full real-time software development is currently underway at our institution. The computer simulation results contained in this paper and our experimental results on human arm and leg tracking (Bachmann, 2000; Bachmann et al., 2001) encourage us to believe that we will succeed in producing a very effective sourceless whole body tracking system prototype in the next several years of our research. As a final remark, we are aware that the linearization of the TQT filter presented in Figure 2, along with the Orthogonal Quaternion Theorem (which allows modeling of orthogonal noise so that the constraint of unit quaternions can be maintained even with sensor noise), permits the scalar gain $k$ to be replaced by a Kalman filter gain matrix. We are not sure of the practicality of such a modification, but this is a topic we intend to pursue (Marins, 2000) and would likewise be pleased to have others join us in this effort

## 9. Acknowledgements

The authors wish to acknowledge the support of the U. S. Army Research Office (ARO) under Proposal No. 40410-MA and the U. S. Navy Modeling and Simulation Management Office (N6M) for making this work possible.

## References

Bachmann, E., McGhee, R., Yun X. & Zyda, M. (2001). "Real-Time Tracking and Display of Human Limb Segment Motions Using Sourceless Sensors and a Quaternion-Based Filtering Algorithm - Part II: Implementation and Calibration," MOVES Academic Group Technical Report NPS-MV-01-003, Naval Postgraduate School, Monterey, CA. http://npsnet.org/~moves/TechReports/NPS-MV-01-003.pdf

Bachmann, E. (2000). *Inertial and Magnetic Angle Tracking of Limb Segments for Inserting Humans into Synthetic Environments*, Ph.D. dissertation, Naval Postgraduate School, Monterey, CA.

Bachmann, E., Duman, I., Usta, U., McGhee, R., Yun, X., & Zyda, M. (1999). "Orientation Tracking for Humans and Robots Using Inertial Sensors", *Proc. of 1999 IEEE International Symposium on Computation in Robotics and Automation, CIRA'99*, Monterey, California, USA, pp. 187 – 194.

Bekey, G., & McGhee, R. (1962). "Gradient Methods for the Optimization of Dynamic System Parameters by Hybrid Computation", *in Computing Methods in Optimization Problems*, ed. by A.V. Balakrishnan and L.W. Neustadt, Academic Press, New York, pp. 305 – 327.

Brown, R. & Hwang, P. (1997). *Introduction to Random Signals and Applied Kalman Filtering*, 3rd Edition, John Wiley and Sons, New York,

Cooke, J., Zyda, M., Pratt, D., & McGhee, R. (1992). "NPSNET: Flight Simulation Modeling Using Quaternions", *Presence: Teleoperators and Virtual Environments*, Vol.1, No. 4, MIT Press, pp. 404 – 420.

Cormen, T., Leiserson, C., & Rivest, R. (1994). *Introduction to Algorithms*, McGraw-Hill, New York,

Everitt, B. (1987). *Introduction to Optimization Methods and Their Application in Statistics*, Chapman and Hall, New York.

Frey, W. (1996). *Application of Inertial Sensors and Flux-Gate Magnetometers to Real-Time Human Body Motion Capture*, M.S. thesis, Naval Postgraduate School, Monterey, CA.

Foxlin, E. (1994). "An Inertial Head-Orientation Tracker with Automatic Drift Compensation for Use with HMD's", *Proc. Virtual Reality Software and Technology*, VRST'94, edited by G. Singh, S.K. Feiner, and D. Thalmann, World Scientific, Singapore. Also see www.isense.com.

Hartley, H. (1961) "The Modified Gauss-Newton Method for the Fitting of Nonlinear Regression Functions by Least Squares", *Technometrics*, Vol. 3, No. 2, pp. 269 – 280.

Henault, G. (1997). *A Computer Simulation Study and Computational Evaluation for a Quaternion Filter for Sourceless Tracking of Human Limb Segment Motion*, M.S. thesis, Naval Postgraduate School, Monterey, CA.

Kuipers, J. (1998). *Quaternions and Rotation Sequences*, Princeton University Press, Princeton, NJ,

Lawrence, A. (1998). *Modern Inertial Technology*, 2nd Edition, Springer-Verlag, New York.

Levine, A. (1971). *Theory of Probability*, Addison-Wesley, Reading, MA.

McGhee, R. (1963). *Identification of Nonlinear Dynamic Systems by Regression Analysis Methods*, Ph.D. Dissertation, University of Southern California,. Available from www.contentville.com.

McGhee, R. (1967). "Some Parameter-Optimization Techniques", Chapter 4.8, *Digital Computer User's Handbook*, ed. by M. Klerer and G.A. Korn, pp. 234 – 255.

McGhee, R., Bachmann, E., & Zyda, M. (2000). "Rigid Body Dynamics, Inertial Reference Frames, and Graphics Coordinate Systems: A Resolution of Conflicting Conventions and Terminology", MOVES Academic Group Technical Report NPS-MV-01-002, Naval Postgraduate School, Monterey, CA.

McGhee, R.B., et al., "An Experimental Study of an Integrated GPS/INS System for Shallow-Water AUV Navigation Systems (SANS)", *Proc. Of 9th International Symposium on Unmanned Untethered Submersible Technology*, Marine Systems Engineering Laboratory, Northeastern University, Sept.25 – 27, 1995, pp. 153 –167.

Meyer, K., Applewhite, H., & Biocca, F. (1992). A Survey of Position Trackers, *Presence: Teleoperators and Virtual Environments*, Vol. 1, No. 2, MIT Press, pp. 173 – 200.

Molet, T., Boulic, R., & Thalman, D., "Human Motion Capture Driven by Orientation Measurements", *Presence: Teleoperators and Virtual Environments*, Vol. 8, No. 2, MIT Press, pp. 187 – 203.

Precision Navigation, Inc., (2000). *TCM2 Compass Product Specifications*, Inc., Santa Rosa, CA95403,. Available at www.precisionnav.com.

Rust, B., & Burrus, W. (1972). *Mathematical Programming and the Numerical Solution of Linear Equations*, Elsevier, New York.

Semwai, S., Hightower, R., & Stansfield, S. (1998). "Mapping Algorithms for Real-Time Control of an Avatar Using Eight Sensors", *Presence: Teleoperators and Virtual Environments*, Vol. 7, No. 1, MIT Press, pp. 1 – 21.

Strang, G. (1988).*Linear Algebra and Its Applications*, 3rd Edition, Harcourt College Publishers, San Diego, CA.

Teegarden, D., Lorenz, G., & Neul, R. (1998). "How to Model and Simulate Microgyroscope Systems", *IEEE Spectrum*, pp. 66 – 75.

Yun, X., et al., (1999). "Testing and Evaluation of an Integrated GPS/INS System for Small AUV Navigation", *IEEE Journal of Oceanic Engineering*, Vol. 24, No. 3, pp. 396 – 404.

## Appendix A: Derivation of X-Matrix for Quaternion Filter

Suppose $q$ is a unit quaternion and $\tilde{q} = \alpha q$, where $\alpha$ is any non-zero scalar. Then from Eq. (15):

$$|\tilde{q}|^2 = \alpha^2 \tag{A-1}$$

and

$$\tilde{q} \otimes v \otimes \tilde{q}^{-1} = \alpha q \otimes v \otimes \frac{\alpha q^*}{\alpha^2} = q \otimes v \otimes q^{-1} \tag{A-2}$$

This result shows that there is no requirement for orientation quaternions to be unit quaternions. As shown in the following paragraph, this fact can be used to derive the $X$ matrix appearing in Figure 1.

Suppose $q = (q_0\ q_1\ q_2\ q_3)$ is an arbitrary non-zero quaternion. Then, by definition,

$$q \otimes q^{-1} = 1 + 0u = (1\ 0\ 0\ 0) \tag{A-3}$$

so from the product rule of differential calculus

$$\left(\frac{\partial q}{\partial q_i}\right) \otimes q^{-1} + q \otimes \left(\frac{\partial q^{-1}}{\partial q_i}\right) = 0 \tag{A-4}$$

and

$$\frac{\partial q^{-1}}{\partial q_i} = -q^{-1} \otimes \left(\frac{\partial q}{\partial q_i}\right) \otimes q^{-1} \tag{A-5}$$

From Figure 1, for the quaternion filter, $y(\hat{q})$ is given by

$$y(\hat{q}) = \left(\hat{q}^{-1} \otimes m \otimes \hat{q}, \hat{q}^{-1} \otimes n \otimes \hat{q}\right)^T \tag{A-6}$$

where it is understood that the comma in this expression denotes concatenation and that only the vector part of the indicated expressions is used. Thus $y(\hat{q})$ is a six-row column vector, the same as $y_0$. Using this result, together with Eq. (A-5) above, it follows from the product rule that

$$\frac{\partial\left(q^{-1} \otimes m \otimes q\right)}{\partial q_i} = -q^{-1} \otimes \frac{\partial q}{\partial q_i} \otimes q^{-1} \otimes m \otimes q + q^{-1} \otimes m \otimes \frac{\partial q}{\partial q_i} \tag{A-7}$$

and similarly for the last three components of $y(\hat{q})$. To complete the derivation of X, it is only necessary to note that, from Eq. (8) and (9),

$$\frac{\partial q}{\partial q_0} = \frac{\partial q}{\partial w} = \begin{pmatrix}1 & 0 & 0 & 0\end{pmatrix} = 1 \tag{A-8}$$

$$\frac{\partial q}{\partial q_1} = \frac{\partial q}{\partial x} = \begin{pmatrix}0 & 1 & 0 & 0\end{pmatrix} = i \tag{A-9}$$

$$\frac{\partial q}{\partial q_2} = \frac{\partial q}{\partial y} = \begin{pmatrix}0 & 0 & 1 & 0\end{pmatrix} = j \tag{A-10}$$

$$\frac{\partial q}{\partial q_3} = \frac{\partial q}{\partial z} = \begin{pmatrix}0 & 0 & 0 & 1\end{pmatrix} = k \tag{A-11}$$

Now if it is recognized that each column of $X$ can be written as a six dimensional vector, then Eq. (A-7) through (A-11) define $X$. ANSI Common Lisp code for computing $X$ is available at http://npsnet.org/~bachmann/research.htm, and provides a convenient executable specification for the details of this result. This code also includes a means of evaluating the $X$ matrix by numerical differentiation of the computed measurement vector, $y(\hat{q})$. These two methods give essentially identical results, lending considerable credence to both the above analysis and the associated Lisp code.

## Appendix B: Orthogonal Quaternion Theorem

Theorem: Let *p* and *q* be any two quaternions whose dot product is equal to 0. Such quaternions are said to be *orthogonal*. For all such *p* and *q*, $p = q \otimes v$ where *v* is a unique vector and is given by $v = q^{-1} \otimes p$.

Proof: If *q* and *v* are written using flag notation, then

$$q = q_0 + i\,q_1 + j\,q_2 + k\,q_3 \tag{B-1}$$

and

$$v = 0 + iv_1 + jv_2 + kv_3 \tag{B-2}$$

Multiplying using flag algebra, and collecting terms, evidently:

$$\begin{aligned} p = q \otimes v = &-(q_1v_1 + q_2v_2 + q_3v_3) + i(q_0v_1 + q_2v_3 - q_3v_2) \\ &+ j(q_0v_2 - q_1v_3 + q_3v_1) + k(q_0v_3 + q_1v_2 - q_2v_1) \end{aligned} \tag{B-3}$$

Thus, the dot product of $q$ and $p$ is given by

$$\begin{aligned} q \bullet p = &-q_0q_1v_1 - q_0q_2v_2 - q_0q_3v_3 + q_1q_0v_1 + q_1q_2v_3 - q_1q_3v_2 \\ &+ q_2q_0v_2 - q_2q_1v_3 + q_2q_3v_1 + q_3q_0v_3 + q_3q_1v_2 - q_3q_2v_1 = 0 \end{aligned} \tag{B-4}$$

which proves orthogonality. For the second part of the theorem,

$$q^{-1} \otimes p = q^{-1} \otimes q \otimes v = 1 \otimes v = v \tag{B-5}$$

which is unique.

Q.E.D.

## INITIAL DISTRIBUTION LIST

| | | |
|---|---|---|
| 1. | Defense Technical Information Center<br>8725 John J. Kingman Rd., STE 0944<br>Ft. Belvoir, VA 22060-6218 | 2 |
| 2. | Dudley Knox Library, Code 013<br>Naval Postgraduate School<br>Monterey, CA 93943-5100 | 2 |
| 3. | Research Office, Code 09<br>Naval Postgraduate School<br>Monterey, CA 93943-5138 | 1 |